

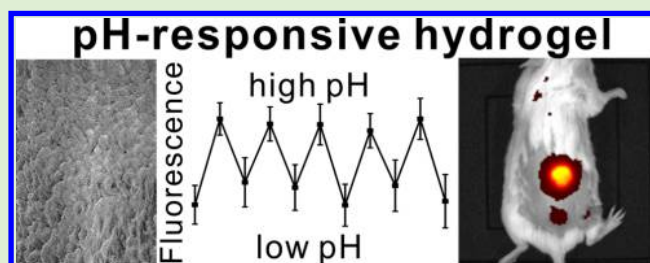
Implantable Tin Porphyrin-PEG Hydrogels with pH-Responsive Fluorescence

Haoyuan Huang,[†] Saurabh Chauhan,[‡] Jumin Geng,[†] Yiru Qin,[†] David F. Watson,[‡] and Jonathan F. Lovell^{*,†}

[†]Department of Biomedical Engineering and [‡]Department of Chemistry, University at Buffalo, State University of New York, Buffalo, New York 14260, United States

Supporting Information

ABSTRACT: Tetracarboxy porphyrins can be polymerized with polyethylene glycol (PEG) diamines to generate hydrogels with intense, near-infrared, and transdermal fluorescence following subcutaneous implantation. Here, we show that the high density porphyrins of the preformed polymer can be chelated with tin via simple incubation. Tin porphyrin hydrogels exhibited increasing emission intensities, ratios, and lifetimes from pH 1 to 10. Tin porphyrin hydrogel emission was strongly reversible and pH responsiveness was observed in the physiological range between pH 6 and pH 8. pH-sensitive emission was detected via noninvasive transdermal fluorescence imaging in vivo following subcutaneous implantation in mice.



INTRODUCTION

Hydrogels are three-dimensional, hydrophilic polymers with a range of potential applications in tissue engineering, drug delivery and biosensing.¹ Frequently, hydrogel biosensors aim to provide a fluorescent output that responds to the presence of chemicals based on changes induced by hydrogel swelling, or by interaction of analytes with encapsulated dyes.² Numerous detection dyes have been immobilized in hydrogel scaffolds for in vivo monitoring of oxygen,^{3,4} glucose,^{5–7} pH,⁸ and even cancer cells.⁹

The pH of physiological fluid plays a critical role in biochemical function. Different body fluids have different pH levels.¹⁰ Metabolic disorders¹¹ and brain tissue damages¹² have been proposed to be diagnosed by unusual pH. Abnormal intracellular pH has been associated with inappropriate cellular functions, which may be implicated to cancers¹³ and Alzheimer's disease.¹⁴

A diversity of molecules can report changes in pH via changes in optical absorption or fluorescence.¹⁵ Several fluorescent dyes have been reported as pH-sensitive optical sensors, such as fluorescein,^{16,17} carbazolyl-pyridinyl conjugate,¹⁸ carbon nanodots,¹⁹ IR or NIR BODIPY dyes,²⁰ and silver nanoclusters.²¹

Porphyrins and related molecules have useful characteristics for theranostic applications.^{22–25} Polyethylene glycol (PEG) is known to modulate in vivo behavior of tetrapyrroles.^{26,27} We previously found that hydrogels could be formed with PEG diamines cross-linked with meso-tetra(4-carboxyphenyl)-porphine (mTCCP) to enable transdermal fluorescence guided hydrogel tracking and surgical resection.²⁸ These bright hydrogels have extreme dye density (5 mM) with minimal

self-quenching, due to the three-dimensional spatial confinement within a PEG mesh. By using the Pd version of mTCCP (Pd mTCCP), the resulting hydrogels had luminescence that decreased at higher oxygen concentrations, thereby creating a biosensor that could be implanted in mice and detect subcutaneous oxygen changes via transdermal phosphorescence imaging.³

Tin porphyrins have been shown in many circumstances to exhibit pH dependent optical properties. SnCl₂-tetraphenyl porphyrin (similar to the free base porphyrin monomer used in porphyrin-PEG hydrogels) has a pH-dependent fluorescence emission that increases from pH 2 to pH 10.²⁹ SnCl₂-tetraphenyl porphyrin membranes demonstrated pH responsiveness.³⁰ Ionic SnCl₂ porphyrins have also been shown to have fluorescence properties that depend on pH.³¹ The fluorescence of tetrapyridyl and tetramethylpyridinium tin porphyrins in solution depends on pH.³² Based on these observations, we hypothesized that tin could be chelated into the porphyrin-PEG hydrogels to confer pH sensitive fluorescence for potential uses in biomedical applications.

MATERIALS AND METHODS

Materials. Unless otherwise specified, reagents were obtained from Sigma. Meso-tetra(4-carboxyphenyl) porphyrin (mTCCP) was obtained from Frontier Scientific. Polyethylene glycol (PEG) 6000 was obtained from Rapp Polymere. *O*-(Benzotriazol-1-yl)-*N,N,N',N'*-tetramethyluronium hexafluorophosphate (HBTU) was obtained from

Received: November 20, 2016

Revised: January 10, 2017

Published: February 1, 2017

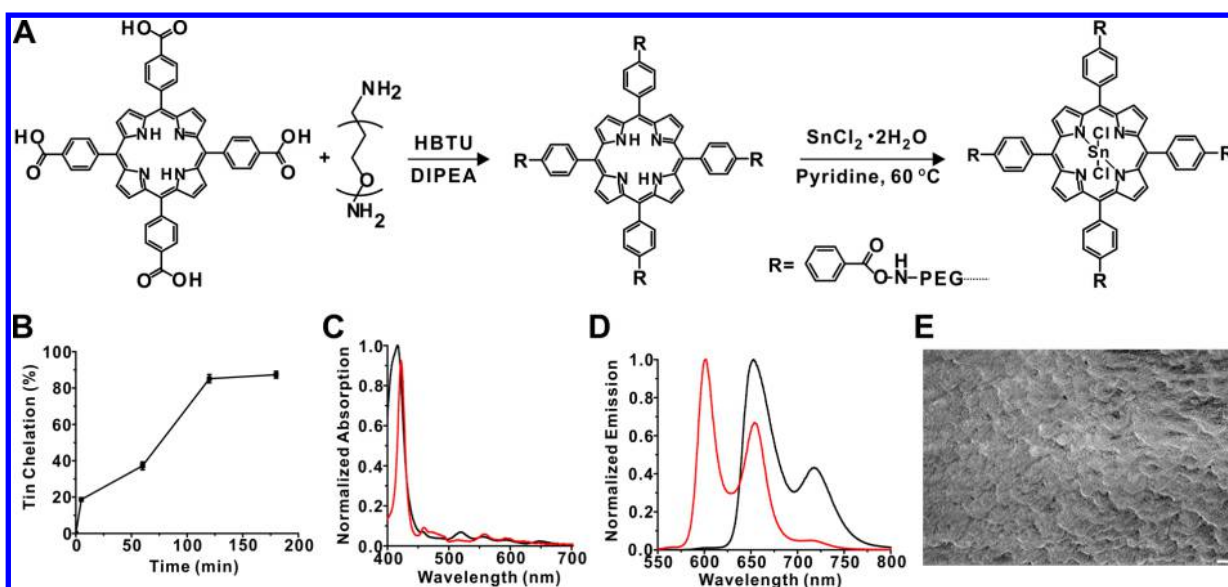


Figure 1. Synthesis of tin-porphyrin-PEG hydrogels. (A) Synthesis of free base mTCPP hydrogel and subsequent tin chelation. (B) Kinetics of SnCl_2 chelation. Data show mean \pm std dev for $n = 3$ separate chelation reactions. (C) Absorbance and (D) fluorescence spectra of 2H-mTCPP (black) and SnCl_2 mTCPP (red) hydrogels. (E) Scanning electron micrograph of a freeze-dried portion of SnCl_2 mTCPP hydrogel. A $1 \mu\text{m}$ scale bar is shown.

Advanced ChemTech. *N,N*-Diisopropylethylamine (DIPEA) was obtained from TCI. Tin(II) chloride dihydrate was obtained from Alfa Aesar. ICR mice were ordered from Harlan Laboratories Inc. Reli Black Nylon-monofilament Sutures (cat # N931) were obtained from MYCO Medical.

mTCPP-PEG Hydrogel Synthesis. mTCPP, PEG-diamine, and HBTU were dissolved separately in *N,N*-dimethylformamide (DMF) to make 15, 30, and 60 mM stock solutions. Equal volumes of mTCPP and HBTU stock solutions were mixed, and $26.6 \mu\text{L}$ of this solution was added to each well of a polypropylene 96-well plate. After adding $2 \mu\text{L}$ of 10% DIPEA in DMF, $13.4 \mu\text{L}$ of PEG-6K solution was added. The total molar ratio of reactants were mTCPP/PEG-6K/HBTU = 1:2:4, which matches their stoichiometric ratio of the reactive groups. After 30 min, excess DMF was added to stop the polymerization and to remove unincorporated reactants.

Synthesis of SnCl_2 -meso-tetra(4-carboxyphenyl)porphine (Sn-mTCPP). The synthetic procedure was based on that reported by Manke et al.³³ Briefly, 200 mg of mTCPP (0.25 mM) was mixed with 113 mg $\text{SnCl}_2 \cdot 2\text{H}_2\text{O}$ (0.50 mM) under nitrogen. A total of 5 mL of anhydrous pyridine was added to the system, and the solution was heated to reflux for 2 h in the dark. After cooling, 30 mL diethyl ether was added and stirred at 4°C in the dark for 12 h. Purple precipitates were collected by filtration and washed with ether, CH_2Cl_2 , water, and ether again. The final product was dried in the vacuo. Yield was 72.1% (178.6 mg). MALDI-MS: $m/z = 908$ ($[\text{M} - 2\text{Cl}]^+$), 943 ($[\text{M} - \text{Cl}]^+$). $^1\text{H NMR}$ (300 MHz, $\text{DMSO}-d_6$): 13.30 (s, 4H, O-H), 9.27 (s, 8H, pyrrole-H), 8.44–8.39 (d, $^3J = 16\text{H}$, ortho-H and meta-H) ppm, as shown in Figure S1.

Chelation of Tin into Preformed mTCPP-PEG Hydrogels. A total of 120 mg of $\text{SnCl}_2 \cdot 2\text{H}_2\text{O}$ was mixed with 24 hydrogel pucks in anhydrous pyridine. The reaction proceeded for 3 h under nitrogen. Then hydrogels were then washed in DMF and water to remove pyridine and unreacted SnCl_2 .

To study the kinetics of tin chelation into the hydrogel, a standard curve was made with different ratios of SnCl_2 mTCPP/mTCPP ranging from 0 to 100%. Then the mixture was polymerized to hydrogels as the same procedure as mTCPP hydrogel synthesis. After the synthesis, fluorescent intensities of hydrogels were tested with TECAN Safire plate reader and the standard curve of fluorescent ratio at 600 and 650 nm to SnCl_2 mTCPP ratio. The standard curve was shown as Figure S2 and $R^2 = 0.99838$. Then, mTCPP hydrogels were post chelated with $\text{SnCl}_2 \cdot 2\text{H}_2\text{O}$ and collected at 0, 5, 60, 120, and 180

min after the temperature reached 60°C . Fluorescent spectra of the hydrogels were scanned and the ratios of fluorescent intensities of hydrogels at 600 and 650 nm were calculated and compared with the standard curve.

Reversible pH Sensitivity of SnCl_2 mTCPP Hydrogels.

SnCl_2 mTCPP hydrogels were put in the well of 96-well plate and fluorescent intensities at 600 nm were tested with plate reader. Then $200 \mu\text{L}$ of different pH 100 mM sodium phosphate solution was added to the well and incubated for 5 min, then pH solutions were removed and fluorescent signals were tested again.

For testing pH sensitivity of hydrogels, they were put in a 96-well plate and treated with acidic or basic pH 100 mM sodium phosphate solutions of indicated pH for 5 min alternately. Fluorescent intensities at 600 nm (for SnCl_2 mTCPP hydrogels) or 650 nm (for 2H mTCPP) were read by the plate reader, and alternating acidic and basic pH solutions were added and fluorescent signals were read after each incubation. Fetal bovine serum (FBS) was added to pH = 4 and 10 100 mM sodium phosphate solutions to make 10% FBS pH buffer. The reversible curve was tested with the same procedure as the experiments without FBS.

Fluorescence Lifetime Decay. Time-resolved photoluminescence decay traces were obtained by a Becker and Hickl Tau-130 time correlated single photon counting (TCSPC) setup. The setup consisted of a vertically polarized pulsed diode laser (BDL 445 SMC) emitting monochromatic radiation at 445 nm at 20 MHz repetition rate. The hydrogel samples were placed on a glass slide inside a four side quartz cuvette, and the cuvette was filled with corresponding buffer solution in which hydrogel was kept in. The emission from the hydrogel samples was collected at 90° from excitation beam and focused into a polychromator coupled to a 16 channel photomultiplier tube (PML 16C). Each channel corresponded to 12.5 nm in the wavelength regime. All measurements were taken at magic-angle conditions by putting a polarizer in the emission channel at 54.7° to the polarization of the excitation beam. A 470 nm long-pass filter was used to avoid scattering of excitation beam from the glass film. A neutral density filter was placed in the excitation pathway to control the intensity of the excitation pulses in such a way that the probability of detection of a photon per excitation pulse was less than 0.01. The decay traces for each sample were collected for 300 s over 4096 time bins with a time resolution of 12.2 ps. Instrument response function (IRF) was acquired by collecting scattered light by silica LUDOX solution. At a laser gain of 20% and detector gain of 90%, the full width

half-maximum (fwhm) of IRF was approximately 220 ps. The collected decay traces were fitted by using Fluofit software by Picoquant.

TRPL decay traces were fitted by using multiexponential reconvolution to eq 1:

$$I(t) = \int_{-\infty}^t \text{IRF}(t') \sum_{i=1}^n A_i \exp\left(-\frac{t-t'}{\tau_i}\right) dt' \quad (1)$$

where $I(t)$ is the intensity of PL decay, $\text{IRF}(t')$ is the instrument response function and A_i is the amplitude of the lifetime component τ_i . The decay profiles were fit with single or biexponential fits, whichever produced a good fit. The goodness of fit was evaluated by distribution of residuals (difference between raw and fit data) around zero and chi-square values. Single and biexponential fits with corresponding chi-square values for representative hydrogels are shown in [Supporting Information](#). Chi-square values between 0.9 and 1.2 were considered as good fits. Intensity weighted average lifetime values $\langle\tau\rangle$ for corresponding decay profiles were calculated according to eq 2:

$$\langle\tau\rangle = \frac{\sum A_i \tau_i^2}{\sum A_i \tau_i} \quad (2)$$

Animal Experiments. Animal experiments were conducted in compliance with University at Buffalo Institutional Animal Care and Use Committee policy. To determine the control group through fluorescent intensity, 85%Cu/15%2H, 90%Cu/10%2H, and 95%Cu/5%2H mTCCP hydrogels were put in 96-well plate with $\text{SnCl}_2\text{mTCCP}$ hydrogels, and the fluorescent photos were tested with an IVIS imaging system with excitation at 640 nm and using the emission signal with the Cy5.5 filter. Mice were anesthetized with 2% (v/v) isoflurane in 100% oxygen carrier gas. Under deep anesthesia, two small incisions were made on the back of mice, then $\text{SnCl}_2\text{mTCCP}$ hydrogels and 95% Cu-mTCCP/5% 2H-mTCCP hydrogels were implanted. The incisions were closed with sutures. Fluorescence images of hydrogels were acquired with an IVIS system with mice under isoflurane anesthesia. For pH-sensitive tests, 200 μL of pH = 4 and 10, 100 mM sodium phosphate solutions were injected subcutaneously near the areas around hydrogels, and fluorescent photos were scanned 1 h post-injection.

RESULTS AND DISCUSSION

Synthesis and Characterization of Tin Porphyrin-PEG Hydrogels. Figure 1A shows the schematic of the synthesis of freebase (2H) mTCCP hydrogels and subsequent chelation with SnCl_2 . 2H-mTCCP hydrogels consist of a highly cross-linked and high density porphyrin-PEG mesh. The polymerization of 2H-mTCCP and PEG was carried out in DMF with HBTU as the coupling condensation agent to form the polyamide. The reaction completed within seconds after adding DIPEA to initiate the reaction. The ratio of mTCCP/PEG/HBTU was 1:2:4, which corresponds to the equimolar ratios of functional groups of tetracarboxylic porphyrin, diamine PEG, and the HBTU acid activator. The resulting hydrogels were washed with DMF to remove the unincorporated reactants.

2H-mTCCP hydrogels were then mixed with $\text{SnCl}_2 \cdot 2\text{H}_2\text{O}$ to post-chelate SnCl_2 to the center of 2H-mTCCP. The post-chelation process took 3 h at 60 °C in pyridine. After the reaction, hydrogels were washed in DMF and then with water several times to remove organic solvents and unreacted SnCl_2 (Figure 1A). The kinetics of the chelation process (Figure 1B) was examined by comparing the fluorescence ratios of the emission intensities at 600 and 650 nm of the reacted hydrogels to a standard curve formed from hydrogels composed of defined ratios of tin and 2H porphyrins (Figure S2). As shown in Figure 1B, the chelation process reached a ~90% yield within 2 h. The absorbance and fluorescence spectra of mTCCP hydrogels and $\text{SnCl}_2\text{mTCCP}$ post chelated hydrogels are shown

in Figure 1C and D, respectively. After tin chelation, the absorbance peak of hydrogels shifts subtly from 420 to 425 nm and fluorescence emission blue shifts from 650 and 720 nm to 600 and 650 nm, resulting in a narrower Stokes shift. Absorbance and fluorescence spectra of tin porphyrin hydrogels were the same whether tin was chelated into preformed hydrogels or whether tin-porphyrins were in the polymerization reaction (Figure S3). Post-chelating tin into preformed freebase hydrogels has the advantage that a single batch of porphyrin hydrogels can be used for multiple applications and was the approach used for this work. Scanning electron microscopy of freeze-dried tin hydrogel is shown in Figure 1D, demonstrating a disordered but highly interconnected $\text{SnCl}_2\text{mTCCP-PEG}$ environment.

pH-Dependent Emission of $\text{SnCl}_2\text{mTCCP}$ Hydrogel.

Axial water molecules of tin(IV) porphyrins can lose protons to yield a hydroxide-coordinated metal compounds to create pH-responsive properties.³⁰ Tin-porphyrin-PEG hydrogels exhibited pH-responsive properties. As shown in Figure 2A, in low pH, fluorescence emission of the tin hydrogels was low. As pH increased toward neutral, fluorescence emission intensities increased. As pH became more basic, the fluorescence increased

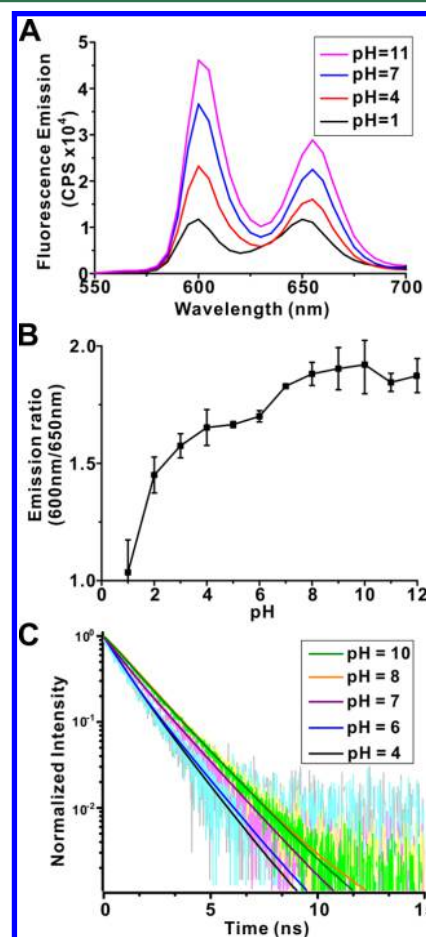


Figure 2. pH sensitivity of tin-porphyrin-PEG hydrogels. (A) Fluorescence spectra of $\text{SnCl}_2\text{mTCCP}$ hydrogels in 100 mM sodium phosphate solutions at indicated pH. (B) Ratio of $\text{SnCl}_2\text{mTCCP}$ hydrogel fluorescence emission intensities at 600 and 650 nm. Data show mean \pm std dev for $n = 3$ separate polymerization reactions and purifications. (C) Fluorescence lifetime at 600 nm emission of $\text{SnCl}_2\text{mTCCP}$ hydrogels in 100 mM sodium phosphate at indicated pH.

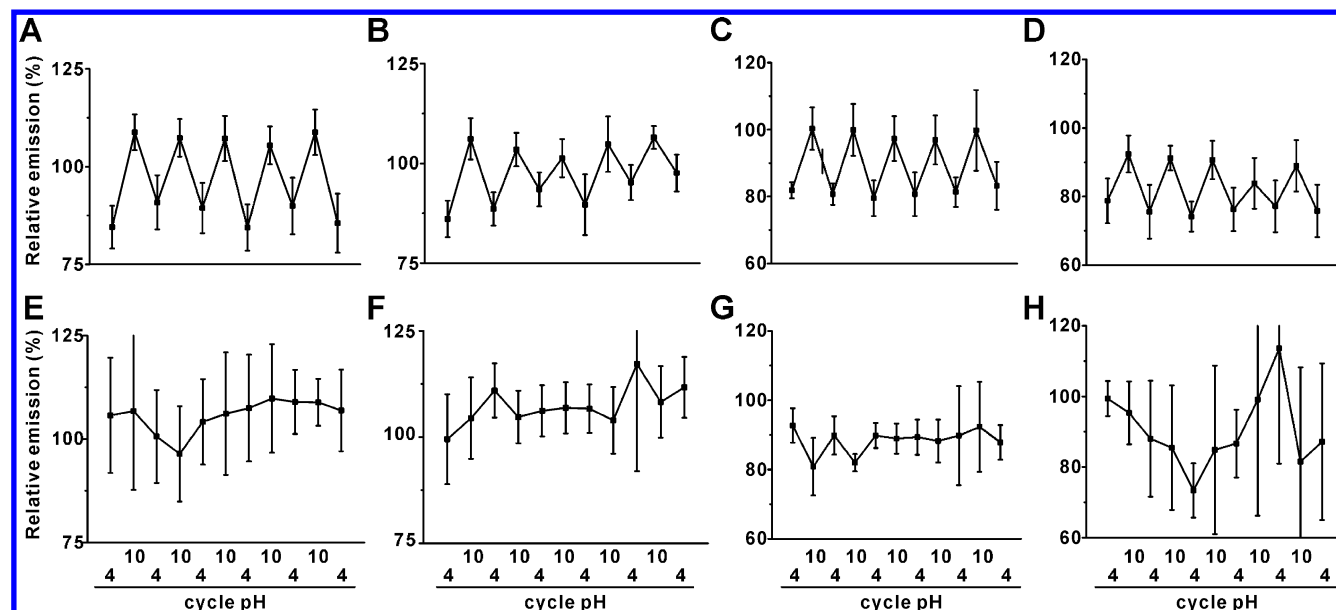


Figure 3. pH-responsive fluorescence reversibility of tin or free base porphyrin hydrogels. Fluorescence emission (normalized to initial emission after formation) of tin porphyrin-PEG hydrogels (top row) or freebase porphyrin-PEG hydrogels (bottom row) placed in 100 mM sodium phosphate solutions of indicated pH (A, E) and after 1 week of storage (B, F). Emission in the presence of 10% fetal bovine serum (FBS) (C, G) and after 1 week of storage in FBS (D, H). Data show mean \pm std dev for $n = 3$ separate polymerization reactions.

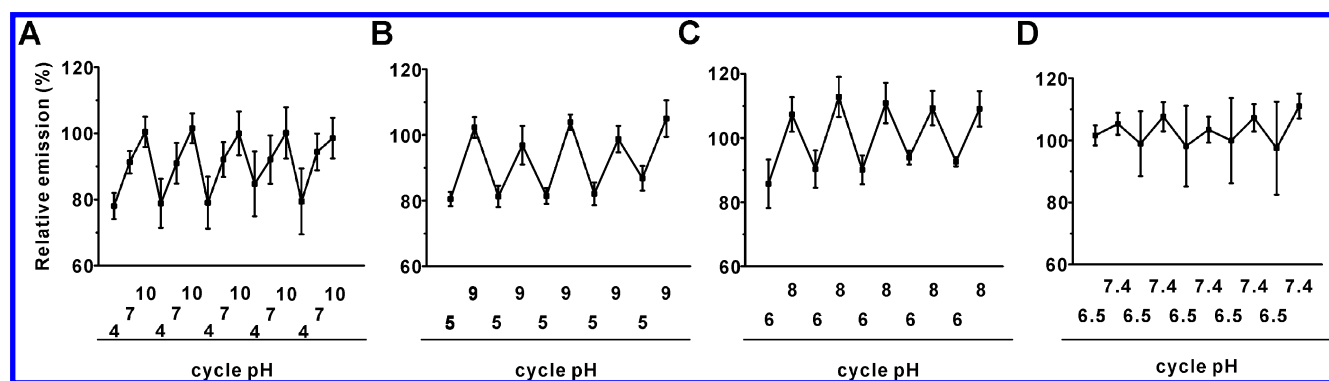


Figure 4. Sensitivity toward intermediate pH by tin-porphyrin-PEG hydrogels. Fluorescence emission (normalized to initial emission after formation) of tin porphyrin-PEG hydrogels placed in 100 mM sodium phosphate solutions of (A) pH = 4, 7, and 10, (B) pH = 5 and 9, and (C) pH = 6 and 8. (D) Fluorescence emission (normalized to initial emission after formation) of tin-porphyrin-PEG hydrogels placed in pH = 6.5 and 7.4 PBS buffer. Data show mean \pm std dev for $n = 3$ separate polymerization reactions.

to a higher level, almost 4-fold higher than at pH = 1. The ratio of the hydrogel fluorescence at 600 and 650 nm offers a quantitative way to gauge pH (Figure 2B). Free base porphyrin hydrogels demonstrated some pH sensitivity (Figure S4), however, this was only at very low pH (i.e., pH < 3) with little physiological relevance. As shown in Figure 2C and Table S1 the average lifetime of tin hydrogels increased from (0.9 ± 0.05) ns to (1.6 ± 0.05) ns, consistent with steady-state emission enhancement as pH increased from 1 to 10.

Reversibility of pH Responsiveness. The pH reversibility of the hydrogels was assessed. As shown in Figure 3A,B, tin-porphyrin-PEG hydrogels exhibited strong fluorescence reversibility between pH = 4 and 10 solutions, even following a week of storage. Such behavior was not observed at all in freebase porphyrin hydrogels lacking tin. The pH reversibility was also assessed in the presence of proteins, since these would be encountered in potential in vivo applications. Based on Figure 3C,D, the SnCl₂mTCCP hydrogels also possessed a similar reversible emission pattern when incubated with 10% fetal

bovine serum in pH = 4 and 10 solutions, while still no reversible pattern was exhibited for hydrogels lacking tin.

Next, tin-porphyrin-PEG hydrogels were assessed for pH responsiveness in more physiologically relevant, intermediate pH ranges. As shown in Figure 4A, fluorescent signals from hydrogels increased from acidic to basic conditions, and the fluorescence at the neutral condition (pH = 7) formed the middle position of the curve. The opposite curve was also observed when pH lowered down from basic system to the acidic circumstance. Then similar tests were performed with a narrower pH range. As shown in Figure 4B,C, hydrogels demonstrated similar reversibility under two pH pairs, pH = 5 and 9 and pH = 6 and 8, respectively. SnCl₂mTCCP hydrogels also demonstrated reversible emission with pH = 6.5 and 7.4 PBS buffer (Figure 4D), demonstrating the potential for pH sensing in physiological relevant conditions. For example, the pH of the extracellular fluid will affect several cellular activation and is known to influence the wound healing process.^{34,35} Therefore, a noninvasive and continuous sensor to monitor pH

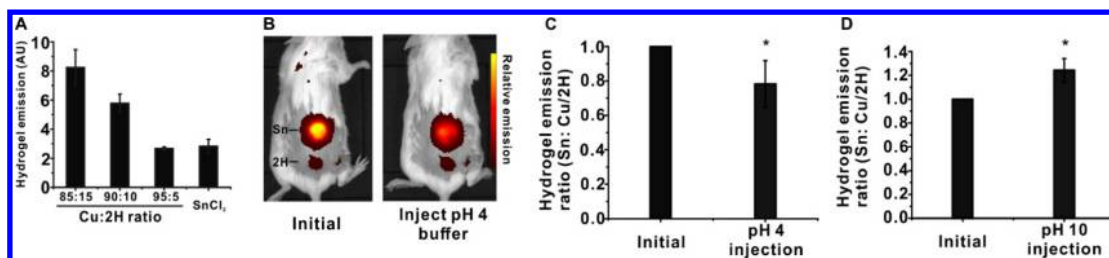


Figure 5. Hydrogel implantation for noninvasive pH sensing in vivo. (A) Fluorescence emission of Cu/2H blended porphyrin hydrogels (non-pH-responsive) relative to tin ones (pH-responsive). (B) Fluorescent images of living mice with an implanted tin hydrogel (top) and Cu/2H hydrogel (bottom), pre- and post-subcutaneous injection with pH = 4, 100 mM sodium phosphate. Relative transdermal fluorescence emission ratios of tin and Cu/2H hydrogels in mice implanted with hydrogels before and after subcutaneous injection with (C) pH = 4 and (D) pH = 10 phosphate solutions. Data show mean \pm std dev for $n = 3$ separate mice; * indicates a statistically significant change based on a two-tailed student's t test ($p < 0.01$).

of subcutaneous extracellular fluid could conceivably help guide certain medical treatments.

In Vivo pH Sensitivity. We next assessed tin-porphyrin-PEG hydrogels for detection of pH changes in mice following subcutaneous implantation. Previously, when investigating Pd-porphyrin hydrogels with oxygen-responsive phosphorescence, we blended nonfluorescent copper mTCPP with freebase mTCPP to make an emission intensity matched control hydrogel.³ In this manner, the two could be implanted simultaneously for ratiometric imaging since only Pd porphyrin hydrogels were oxygen responsive. To this same end, the fluorescence intensities of hydrogels formed with varying ratios of copper and freebase porphyrins were assessed and compared to the SnCl₂mTCPP hydrogels. As shown in Figure 5A, 95:5 Cu/2H-mTCPP hydrogels generated similar fluorescence intensity as SnCl₂mTCPP hydrogels in vitro. Thus, 95:5 Cu-mTCPP/2H-mTCPP hydrogels were coimplanted as a non-responsive companion hydrogel. The hydrogels were implanted subcutaneously on the dorsum of mice. Whole body fluorescence imaging easily detected the hydrogels through the skin of mice (Figure 5B). Unexpectedly, in vivo the Cu/2H companion hydrogel exhibited weaker emission relative to the tin-porphyrin-PEG one but, nevertheless, could be used for ratiometric applications. Following subcutaneous injection of a pH = 4 phosphate solution, the fluorescence of the tin hydrogels decreased, but the Cu/2H one remained constant (Figure 5B). For in vivo pH-responsivity, the changes in fluorescence intensities were demonstrated as the variations of the ratios of the tin to freebase hydrogels, pre- and post-injection with pH = 4 and 10, 100 mM sodium phosphate solutions. As shown in Figure 5C,D, pH = 4 phosphate solution decreased the emission of the tin hydrogel by about 20%, while pH = 10 solutions increased the intensity about 30%, which roughly matches in vitro the pH-responsive pattern.

Mice tolerated tin porphyrin hydrogel implantation and imaging without incident. Tin and tin alloys have been used in routine human life for thousands of years (e.g., in plates and mugs) and are generally safe, whereas organotin compounds containing C–Sn bonds (absent from the hydrogel) are toxic.³⁶ A tin-chelated chlorin, tin etiopurpurin, has been used clinically with intravenous injection for photodynamic therapy.³⁷ Nevertheless, actual toxicity studies would be required to make any conclusions about the safety of the tin porphyrin hydrogels.

CONCLUSION

In this work, a pH-responsive hydrogel was generated by post-chelating SnCl₂ into free base mTCPP hydrogels. This post-

chelation process was simple and effective. Tin porphyrin hydrogels provide a wide pH-responsive range and the potential for quantifying pH of the surrounding environment. The pH responsiveness was fully reversible in aqueous environments and in the presence of biomolecules found in serum. The tin porphyrin hydrogels, with extreme porphyrin density, were bright enough for facile transdermal fluorescence imaging following implantation and responded to changes in pH in vivo. Future work will aim to develop injectable hydrogels to avoid implantation surgery, to develop more quantitative ratiometric approaches and to assess toxicity. We conclude that tin porphyrin hydrogels hold potential for noninvasive, long-term measurement of pH values inside the body.

ASSOCIATED CONTENT

Supporting Information

The Supporting Information is available free of charge on the ACS Publications website at DOI: 10.1021/acs.biomac.6b01715.

Supporting Figures 1–4 and Supporting Table 1, showing NMR, ratiometric standard curve, spectra, and free base porphyrin data (PDF).

AUTHOR INFORMATION

Corresponding Author

*E-mail: jflovell@buffalo.edu.

ORCID

David F. Watson: 0000-0003-1203-2811

Jonathan F. Lovell: 0000-0002-9052-884X

Notes

The authors declare no competing financial interest.

ACKNOWLEDGMENTS

This work was supported by the National Institutes of Health (DP5OD017898).

REFERENCES

- Hoffman, A. S. Hydrogels for biomedical applications. *Adv. Drug Delivery Rev.* **2012**, *64*, 18–23.
- Peppas, N. A.; Van Blarcom, D. S. Hydrogel-based biosensors and sensing devices for drug delivery. *J. Controlled Release* **2016**, *240*, 142–50.
- Huang, H.; Song, W.; Chen, G.; Reynard, J. M.; Ohulchanskyy, T. Y.; Prasad, P. N.; Bright, F. V.; Lovell, J. F. Pd-Porphyrin-Cross-Linked

Implantable Hydrogels with Oxygen-Responsive Phosphorescence. *Adv. Healthcare Mater.* **2014**, *3* (6), 891–6.

(4) Zhang, L.; Su, F.; Buizer, S.; Lu, H.; Gao, W.; Tian, Y.; Meldrum, D. A dual sensor for real-time monitoring of glucose and oxygen. *Biomaterials* **2013**, *34* (38), 9779–88.

(5) Nichols, S. P.; Koh, A.; Storm, W. L.; Shin, J. H.; Schoenfisch, M. H. Biocompatible Materials for Continuous Glucose Monitoring Devices. *Chem. Rev.* **2013**, *113* (4), 2528–49.

(6) Heo, Y. J.; Shibata, H.; Okitsu, T.; Kawanishi, T.; Takeuchi, S. Long-term in vivo glucose monitoring using fluorescent hydrogel fibers. *Proc. Natl. Acad. Sci. U. S. A.* **2011**, *108* (33), 13399–403.

(7) Shibata, H.; Heo, Y. J.; Okitsu, T.; Matsunaga, Y.; Kawanishi, T.; Takeuchi, S. Injectable hydrogel microbeads for fluorescence-based in vivo continuous glucose monitoring. *Proc. Natl. Acad. Sci. U. S. A.* **2010**, *107* (42), 17894–8.

(8) Richter, A.; Paschew, G.; Klatt, S.; Lienig, J.; Arndt, K.-F.; Adler, H.-J. Review on Hydrogel-based pH Sensors and Microsensors. *Sensors* **2008**, *8* (1), 561.

(9) Wang, H.; Mao, D.; Wang, Y.; Wang, K.; Yi, X.; Kong, D.; Yang, Z.; Liu, Q.; Ding, D. Biocompatible fluorescent supramolecular nanofibrous hydrogel for long-term cell tracking and tumor imaging applications. *Sci. Rep.* **2015**, *5*, 16680.

(10) Evans, D. F.; Pye, G.; Bramley, R.; Clark, A. G.; Dyson, T. J.; Hardcastle, J. D. Measurement of gastrointestinal pH profiles in normal ambulant human subjects. *Gut* **1988**, *29* (8), 1035–41.

(11) Jin, W.; Jiang, J.; Wang, X.; Zhu, X.; Wang, G.; Song, Y.; Bai, C. Continuous intra-arterial blood pH monitoring in rabbits with acid-base disorders. *Respir. Physiol. Neurobiol.* **2011**, *177* (2), 183–8.

(12) Grant, S. A.; Bettencourt, K.; Krulevitch, P.; Hamilton, J.; Glass, R. In vitro and in vivo measurements of fiber optic and electrochemical sensors to monitor brain tissue pH. *Sens. Actuators, B* **2001**, *72* (2), 174–9.

(13) Georgiev, N. I.; Bryaskova, R.; Tzoneva, R.; Ugrinova, I.; Detrembleur, C.; Miloshev, S.; Asiri, A. M.; Qusti, A. H.; Bojinov, V. B. A novel pH sensitive water soluble fluorescent nanomicellar sensor for potential biomedical applications. *Bioorg. Med. Chem.* **2013**, *21* (21), 6292–302.

(14) Davies, T. A.; Fine, R. E.; Johnson, R. J.; Levesque, C. A.; Rathbun, W. H.; Seetoo, K. F.; Smith, S. J.; Strohmeier, G.; Volicer, L.; Delva, L.; Simons, E. R. Non-age Related Differences in Thrombin Responses by Platelets from Male Patients with Advanced Alzheimer's Disease. *Biochem. Biophys. Res. Commun.* **1993**, *194* (1), 537–43.

(15) Wencel, D.; Abel, T.; McDonagh, C. Optical Chemical pH Sensors. *Anal. Chem.* **2014**, *86* (1), 15–29.

(16) Schreml, S.; Meier, R. J.; Weiß, K. T.; Cattani, J.; Flittner, D.; Gehmert, S.; Wolfbeis, O. S.; Landthaler, M.; Babilas, P. A sprayable luminescent pH sensor and its use for wound imaging in vivo. *Exp. Dermatol.* **2012**, *21* (12), 951–3.

(17) Lee, M. H.; Han, J. H.; Lee, J. H.; Park, N.; Kumar, R.; Kang, C.; Kim, J. S. Two-Color Probe to Monitor a Wide Range of pH Values in Cells. *Angew. Chem., Int. Ed.* **2013**, *52* (24), 6206–9.

(18) Yang, Z.; Qin, W.; Lam, J. W. Y.; Chen, S.; Sung, H. H. Y.; Williams, I. D.; Tang, B. Z. Fluorescent pH sensor constructed from a heteroatom-containing luminogen with tunable AIE and ICT characteristics. *Chem. Sci.* **2013**, *4* (9), 3725–30.

(19) Shi, W.; Li, X.; Ma, H. A Tunable Ratiometric pH Sensor Based on Carbon Nanodots for the Quantitative Measurement of the Intracellular pH of Whole Cells. *Angew. Chem.* **2012**, *124* (26), 6538–41.

(20) Ni, Y.; Wu, J. Far-red and near infrared BODIPY dyes: synthesis and applications for fluorescent pH probes and bio-imaging. *Org. Biomol. Chem.* **2014**, *12* (23), 3774–91.

(21) Qu, F.; Li, N. B.; Luo, H. Q. Highly Sensitive Fluorescent and Colorimetric pH Sensor Based on Polyethylenimine-Capped Silver Nanoclusters. *Langmuir* **2013**, *29* (4), 1199–205.

(22) Huang, H.; Song, W.; Rieffel, J.; Lovell, J. F. Emerging applications of porphyrins in photomedicine. *Front. Phys.* **2015**, *3* (23), n/a.

(23) Zhang, Y.; Lovell, J. F. Porphyrins as Theranostic Agents from Prehistoric to Modern Times. *Theranostics* **2012**, *2* (9), 905–15.

(24) Huang, H.; Lovell, J. F. Advanced Functional Nanomaterials for Theranostics. *Adv. Funct. Mater.* **2017**, *27* (2), 1603524.

(25) Zhang, Y.; Lovell, J. F. Recent applications of phthalocyanines and naphthalocyanines for imaging and therapy. *WIREs: Nanomed. Nanobiotechnol.* **2017**, *9* (1), e1420.

(26) Huang, H.; Wang, D.; Zhang, Y.; Zhou, Y.; Geng, J.; Chitgupi, U.; Cook, T. R.; Xia, J.; Lovell, J. F. Axial PEGylation of Tin Octabutoxy Naphthalocyanine Extends Blood Circulation for Photoacoustic Vascular Imaging. *Bioconjugate Chem.* **2016**, *27* (7), 1574–8.

(27) Huang, H.; Hernandez, R.; Geng, J.; Sun, H.; Song, W.; Chen, F.; Graves, S. A.; Nickles, R. J.; Cheng, C.; Cai, W.; Lovell, J. F. A porphyrin-PEG polymer with rapid renal clearance. *Biomaterials* **2016**, *76*, 25–32.

(28) Lovell, J. F.; Roxin, A.; Ng, K. K.; Qi, Q.; McMullen, J. D.; DaCosta, R. S.; Zheng, G. Porphyrin-Cross-Linked Hydrogel for Fluorescence-Guided Monitoring and Surgical Resection. *Biomacromolecules* **2011**, *12* (9), 3115–8.

(29) Grigg, R.; Norbert, W. D. J. A. The proton-controlled fluorescence of aminomethyltetraphenylporphyrin-tin(IV) derivatives. *J. Chem. Soc., Chem. Commun.* **1992**, No. 18, 1298–300.

(30) Chaniotakis, N. A.; Park, S. B.; Meyerhoff, M. E. Salicylate-selective membrane electrode based on tin(IV)-tetraphenylporphyrin. *Anal. Chem.* **1989**, *61* (6), 566–70.

(31) George, R. C.; Egharevba, G. O.; Nyokong, T. Spectroscopic studies of nanostructures of negatively charged free base porphyrin and positively charged tin porphyrins. *Polyhedron* **2010**, *29* (5), 1469–74.

(32) Delmarre, D.; Veret-Lemarinier, A.-V.; Bied-Charreton, C. Spectroscopic properties of Sn(IV) tetrapyrrolyl and tetramethylpyridinium porphyrins in solution and in sol–gel matrices. *J. Lumin.* **1999**, *82* (1), 57–67.

(33) Manke, A.-M.; Geisel, K.; Fetzer, A.; Kurz, P. A water-soluble tin(IV) porphyrin as a bioinspired photosensitizer for light-driven proton-reduction. *Phys. Chem. Chem. Phys.* **2014**, *16* (24), 12029–42.

(34) Schreml, S.; Szeimies, R. M.; Karrer, S.; Heinlin, J.; Landthaler, M.; Babilas, P. The impact of the pH value on skin integrity and cutaneous wound healing. *J. Eur. Acad. Dermatol. Venereol.* **2010**, *24* (4), 373–8.

(35) Schreml, S.; Meier, R. J.; Kirschbaum, M.; Kong, S. C.; Gehmert, S.; Felthaus, O.; Küchler, S.; Sharpe, J. R.; Wöltje, K.; Weiß, K. T. Luminescent dual sensors reveal extracellular pH-gradients and hypoxia on chronic wounds that disrupt epidermal repair. *Theranostics* **2014**, *4* (7), 721–35.

(36) Rüdell, H. Case study: bioavailability of tin and tin compounds. *Ecotoxicol. Environ. Saf.* **2003**, *56* (1), 180–9.

(37) Josefsen, L. B.; Boyle, R. W. Photodynamic Therapy and the Development of Metal-Based Photosensitizers. *Met. Based Drugs* **2008**, *2008*, 276109.